Surface Lattice Dynamics of Silver. II. Low-Energy Electron Thermal Diffuse Scattering*

JAMES T. MCKINNEY,† EDWIN R. JONES,‡ AND MAURICE B. WEBB
University of Wisconsin, Madison, Wisconsin
(Received 29 March 1967)

Intensity measurements of the diffracted current in the low-energy electron diffraction from the (111) surface of silver show broad wings associated with the Bragg peaks. These wings have been identified as the thermal diffuse scattering. The observed intensity has been compared with model calculations for kinematic scattering of nonpenetrating radiation, using a Debye spectrum of vibrational modes. After the effects of the scattering factor and a temperature-independent background are accounted for, the data agree with the predictions of the model in the following ways: (i) Throughout nearly the entire Brillouin zone the intensity was inversely proportional to the distance to the nearest reciprocal-lattice rod. (ii) The ratio of the diffuse intensity to the peak intensity was proportional to temperature. (iii) The same ratio was proportional to the square of the length of the scattering vector. (iv) The ratio of the integrated intensities in the thermal diffuse scattering and in the peak was approximately equal to the exponent in the Debye-Waller factor. Refinements of the model to include qualitatively the penetration of the incident electrons and the free-surface elastic boundary conditions yield additional features that are only suggested in the data. However, to within the uncertainties in this analysis and the experiments, the results for the close-packed surface of silver can be understood in terms of an elastic continuum, and are consistent with the Debye-Waller factor for low-energy electrons.

INTRODUCTION

In an earlier paper (hereafter referred to as I), measurements of the Debye-Waller factor for the low-energy electron diffraction from the (111) surface of Ag were reported.[1] In that work the penetration of the elastically scattered electrons was estimated and the effective Debye temperatures were measured. These data were analyzed using a kinematic description of the diffraction. It was concluded that the penetration of the coherently scattered electrons could be approximately described by a linear absorption coefficient $\mu=1.4\,E^{-1/2}$ Å^{-1} for energies above 120 eV. The energy dependence of the effective Debye temperature indicated that the mean square of the normal component of the displacement of the surface atoms from their equilibrium positions is 2.0±0.2 times that for the bulk atoms and that this excess surface amplitude decreases with depth approximately as e^{-n} where n labels the atomic planes. In the course of these experiments it was discovered that the profile of a diffraction peak shows broad wings extending throughout the Brillouin zone.[2] It is the purpose of this paper to establish that these wings are the thermal diffuse scattering and to demonstrate the properties of this scattering for the case of slightly penetrating radiation.

In the kinematic description of diffraction, the scattered intensity for unit incident intensity is given by[3]

$$I(\mathbf{S})=|f_0|^2e^{-\langle(\mathbf{S}\cdot\mathbf{u})^2\rangle}\{I_0(\mathbf{S})+\sum_{ij}e^{i\mathbf{S}\cdot(\mathbf{r}_i-\mathbf{r}_j)}\langle(\mathbf{S}\cdot\mathbf{u}_i)(\mathbf{S}\cdot\mathbf{u}_j)\rangle\}\,, \quad (1)$$

where $\mathbf{S}$ is the scattering vector equal to $\mathbf{k}-\mathbf{k}_0$ ($\mathbf{k}$ and $\mathbf{k}_0$ are the wave vectors of the scattered and incident waves), $\mathbf{u}_i$ is the displacement of the ith atom from its equilibrium position, and $I_0(\mathbf{S})$ is the interference function of the rigid lattice. $\langle\ \rangle$ represents the time average. The first term in the braces is the Bragg scattering and the second is the thermal diffuse scattering. Each of these terms is multiplied by the Debye Waller factor $e^{-\langle(\mathbf{S}\cdot\mathbf{u})^2\rangle}$. When the displacements are expanded in the normal modes and inserted, the thermal diffuse term can be written

$$I_2(\mathbf{S})=\tfrac{1}{4}|f_0|^2e^{-\langle(\mathbf{S}\cdot\mathbf{u})^2\rangle}\sum_{\mathbf{q}z}\langle u_{\mathbf{q}z}{}^2\rangle(\mathbf{S}\cdot\mathbf{e}_{\mathbf{q}z})^2I_0(\mathbf{S}\pm\mathbf{q})\,, \quad (2)$$

where $\mathbf{q}$ is the phonon wave vector, z is a polarization index, $\mathbf{e}_{\mathbf{q}z}$ is the unit polarization vector and $\langle u_{\mathbf{q}z}{}^2\rangle$ is the thermal average of the square of the amplitude of the $\mathbf{q}z$th mode. I_0 is a set of very sharp peaks centered at reciprocal-lattice points, and consequently, $I_0(\mathbf{S}\pm\mathbf{q})$ will have an appreciable value only when $\mathbf{S}\pm\mathbf{q}=\mathbf{G}$ where $\mathbf{G}$ is a reciprocal-lattice vector. Thus the diffuse scattering gives a measure of the component along $\mathbf{S}$ of the mean-square amplitude of those phonons satisfying this condition. When the amplitude of the phonons is evaluated in the high-temperature limit for a Debye spectrum and inserted into Eq. (1),

$$I_2(\mathbf{S})\propto\frac{|\mathbf{S}|^2kT}{mc^2|\mathbf{S}-\mathbf{G}|^2}\,, \quad (3)$$

* This work supported by the U. S. Air Force Office of Scientific Research Grant No. AF-AFOSR-51-63/AF-AFOSR-51-66.
† Present address: U. S. Steel Research Center, Monroeville, Pennsylvania.
‡ Present address: University of South Carolina, Columbia, South Carolina.
[1] E. R. Jones, J. T. McKinney, and M. B. Webb, Phys. Rev. **151**, 467 (1966).
[2] J. T. McKinney, E. R. Jones, and M. B. Webb, Bull. Am. Phys. Soc. **10**, 324 (1965).
[3] R. W. James, *The Optical Principles of the Diffraction of X-Rays* (G. Bell and Sons, London, 1962).

where m is the mass of the atom and c is an average sound velocity. We have averaged over the polarization terms $(\mathbf{S}\cdot\mathbf{e}_{qz})^2$ and the velocities of phonons with different polarizations. The scattering is then a series of broad peaks centered at reciprocal lattice points and decreasing as the reciprocal of the square of the distance to these points. In the next section of this paper we present the modifications of Eq. (3) necessary for nonpenetrating radiation.

Aldag and Stern[4] have reported observations of diffuse scattering from the (110) surface of W which they have attributed to the thermal diffuse scattering. Photometric measurements of integrated intensities as a function of temperature support their suggestions.

Huber[5] has calculated the diffuse scattering for nonpenetrating radiation from an elastic continuum taking into account the free-surface boundary conditions. Wallis and Maradudin[6] have calculated the diffuse scattering from a model of the discrete lattice, again for nonpenetrating radiation.

To provide a framework for the discussion of the experimental investigation of the thermal diffuse scattering, in the first section of this paper we calculate the scattering for the simplest possible model. In the next section, we describe the experiments. We then discuss the angular dependence, temperature dependence, energy dependence, and integrated intensities of the diffuse scattering and compare these with the predictions of the simple model. Finally we briefly discuss features which are expected from more complete analyses which include the finite penetration of the electrons into the crystal and more detailed consideration of the lattice dynamics of the surface.

THERMAL DIFFUSE SCATTERING OF LOW-ENERGY ELECTRONS

We wish to modify Eq. (2) for the case of low-energy electron diffraction. The analysis will be done in a kinematic approximation, which is known to be insufficient to explain many features of the low-energy electron diffraction. However, here we shall be concerned only with the scattered intensities associated with diffraction maxima arising from the residual third Laue equation and then only with the temperature-dependent part of this scattering. Thus it is hoped that the kinematic contributions to the scattering will be dominant. As in I, the justification for this hope lies in the consistency of the results.

We assume that the surface structure is that obtained by terminating the bulk structure along a plane. We also assume that only the atoms in the outermost layer contribute to the scattering. The appropriate reciprocal lattice is then a family of rods (h,k) normal to the crystal surface and $I_0(\mathbf{S})$ is nearly zero everywhere except in the immediate vicinity of these rods.

[4] J. Aldag and R. M. Stern, Phys. Rev. Letters 14, 857 (1965).
[5] D. L. Huber, Phys. Rev. 153, 772 (1967).
[6] R. F. Wallis and A. A. Maradudin, Phys. Rev. 148, 962 (1966).

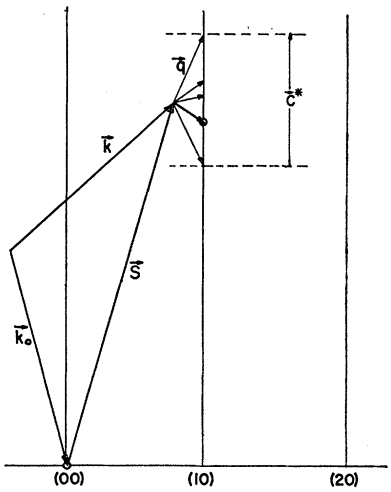

FIG. 1. Thermal diffuse scattering from a surface. $\mathbf{k}$ and $\mathbf{k}_0$ are the wave vectors of the scattered and incident beams; $\mathbf{S}=\mathbf{k}-\mathbf{k}_0$; $\mathbf{C}^*$ is a basis vector of the reciprocal lattice of the bulk structure; $\mathbf{q}$ is a phonon wave vector. All phonons for which $\mathbf{q}$ reaches from the tip of $\mathbf{S}$ to a reciprocal rod contribute to the thermal diffuse scattering at $\mathbf{S}$.

Thus in Eq. (2) many more terms in the sum over phonons contribute to $I_2(\mathbf{S})$, as illustrated in Fig. 1. For a particular value of $\mathbf{S}$, there will be a contribution from all those phonons whose wave vector reaches from $\mathbf{S}$ to the nearest reciprocal-lattice rod, that is, from those phonons for which $q_{||}=S_{||}-G_{||}$, where the subscripts indicate the components parallel to the surface and $\mathbf{G}$ is a reciprocal-lattice vector for the two dimensional structure. When the sum over these terms is replaced by an integral over the Brillouin zone centered at $\mathbf{S}$,

$$I_2(\mathbf{S})=\tfrac{1}{4}|f_0|^2e^{-2M}\sum_z\left(\frac{Nd}{2\pi}\right)^3\int_{\text{zone}}(\mathbf{S}\cdot\mathbf{e}_{qz})^2 \times\langle u_{qz}^2\rangle I_0(\mathbf{S}\pm\mathbf{q})d\mathbf{q}, \quad (4)$$

where d is the lattice spacing and $(Nd/2\pi)^3$ is the density of phonon states for a crystal with N atoms on an edge. e^{-2M} is the Debye-Waller factor.

To proceed, we need to evaluate the $\langle u_{qz}^2\rangle$, which are actually determined by the free-surface elastic boundary conditions. This is the burden of the work of Refs. 5 and 6. To display the general features of the thermal diffuse scattering, we shall assume simply that the thermal motion of the surface atoms can be described by a Debye spectrum. We shall account qualitatively for surface modes in a subsequent paragraph and in a later section discuss effects expected from the refinement of this model. Under this assumption

$$I_2(\mathbf{S})=\tfrac{1}{2}|f_0|^2e^{-2M}\left(\frac{Nd}{2\pi}\right)^3\sum_z\int_{q_\perp}\int_{q_{||}}(\mathbf{S}\cdot\mathbf{e}_{qz})^2 \times\frac{2kT}{Nmc_z^2|\mathbf{q}|^2}I_0(\mathbf{S}+\mathbf{q})dq_{||}dq_\perp. \quad (5)$$

Here it has been recognized that the integral over $I_0(\mathbf{S}+\mathbf{q})$ is the same as over $I_0(\mathbf{S}-\mathbf{q})$.$\langle u_{qz}^2\rangle$ has been replaced by its value in the high-temperature limit. The integral over a plane perpendicular to a reciprocal-lattice rod is[3] $N^2(2\pi/d)^2$, and thus

$$I_2(\mathbf{S})=|f_0|^2e^{-2M}\frac{N^2kTd}{2\pi mc^2}|\mathbf{S}|^2\int_{-\pi/a}^{\pi/a}dq_\perp/(|S_{||}-G_{||}|^2+q_\perp^2).$$

Here the phonon velocities and the factor $(\mathbf{S}\cdot\mathbf{e}_{qz})^2$ have both been replaced by averages over polarizations. Integration gives

$$I_2(\mathbf{S})=|f_0|^2(e^{-2M})\frac{N^2kTd|\mathbf{S}|^2}{\pi mc^2}\frac{1}{|S_{||}-G_{||}|}\times\tan^{-1}\frac{\pi}{d|S_{||}-G_{||}|},\quad(6)$$

or for $|S_{||}-G_{||}|\ll\pi/d$,

$$I_2(\mathbf{S})\approx|f_0|^2(e^{-2M})\frac{N^2kTd|\mathbf{S}|^2}{2mc^2}\frac{1}{|S_{||}-G_{||}|}.\quad(7)$$

Throughout much of the zone the scattering falls as the reciprocal of the distance to the nearest rod. Near the zone boundary this model is inadequate and the diffuse scattering will be more complicated both because of the phonon dispersion relation of the discrete lattice and because of the modulation of $I_0(\mathbf{S})$ along the reciprocal-lattice rods. Therefore we will be concerned first with the region where the scattering is expected to go as $|S_{||}-G_{||}|^{-1}$.

In the above integration we have included only bulk modes. Surface modes will also contribute to the displacement of the surface atoms and so to the diffuse scattering. For these modes, which have $q_\perp=0$, there is no integration over $q_\perp$; however, the angular dependence of the scattering from these modes will be proportional to $|S_{||}-G_{||}|^{-1}$ just as for the bulk modes. This is because the amplitude of the displacements due to the surface modes decreases with depth into the crystal in a distance like the wavelength. Therefore the number of atoms participating in the mode goes as $|\mathbf{q}|^{-1}$, and by equipartition the $\langle u_{qz}^2\rangle$ contain an additional factor of $|\mathbf{q}|=|S_{||}-G_{||}|$ compared to Eq. (3). The contribution to the scattering then goes as $|S_{||}-G_{||}|^{-1}$ as for bulk modes.

Equations (6) and (7) predict several features of the thermal diffuse scattering which may be observed experimentally:

1. The scattered intensity should be inversely proportional to the distance to the nearest reciprocal lattice rod.

2. The ratio of the intensity of the thermal diffuse scattering to the intensity of the associated Bragg peak should be proportional to the temperature.

3. The same ratio should be proportional to the square of the magnitude of the scattering vector.

4. As will be demonstrated in the next paragraph, the ratio of the integrated intensities in the thermal diffuse scattering and the associated Bragg peak should be approximately equal to the exponent in the Debye-Waller factor, $2M$.

Since Eq. (5) for the diffuse intensity contains experimental parameters and unknown constants describing the crystal, it is more convenient to consider the ratio of the diffuse and Bragg intensities. From Eq. (2) we obtain

$$R=\frac{\int I_2(\mathbf{S})d\Omega}{\int I_1(\mathbf{S})d\Omega}=\frac{\frac{1}{4}\sum_{qz}\langle u_{qz}^2\rangle\int(\mathbf{S}\cdot\mathbf{e}_{qz})^2I_0(\mathbf{S}\pm\mathbf{q})d\Omega}{\int I_0(\mathbf{S})d\Omega},\quad(8)$$

where the integrals are to be taken over a plane through the Brillouin zone. Since $I_0(\mathbf{S})$ is sharply peaked, $(\mathbf{S}\cdot\mathbf{e}_{qz})^2$ can be taken outside the integral as $[(\mathbf{G}\mp\mathbf{q})\cdot\mathbf{e}_{qz}]^2$. Then

$$R=\tfrac{1}{4}\sum_{qz}\langle u_{qz}^2\rangle\{[(\mathbf{G}-\mathbf{q})\cdot\mathbf{e}_{qz}]^2+[(\mathbf{G}+\mathbf{q})\cdot\mathbf{e}_{qz}]^2\},\quad(9)$$

and

$$R=\tfrac{1}{2}\sum_{qz}\langle u_{qz}^2\rangle\{(\mathbf{G}\cdot\mathbf{e}_{qz})^2+(\mathbf{q}\cdot\mathbf{e}_{qz})^2\}.\quad(10)$$

But since

$$\tfrac{1}{2}\sum_{qz}(\mathbf{S}\cdot\mathbf{e}_{qz})^2\langle u_{qz}^2\rangle=2M,\qquad R=2M[1+\Delta],\quad(11)$$

where Δ is a term of the order of $|\mathbf{q}|^2/|\mathbf{G}|^2$, which is always less than unity and goes toward zero for higher-order reflections. In Eq. (11) the value of $2M$ is that appropriate to the surface layers as determined by the Debye-Waller effect for the low-energy electrons in I. This result is independent of the size of the coherently scattering domain and of detailed assumptions about the phonon spectrum.

The primary purpose of this paper is to compare the experimental observations with these results.

RESULTS

The apparatus and procedures were described in I.

Angular Dependence

We now discuss the dependence of the diffuse intensity on the distance to the nearest reciprocal-lattice rod. Figure 2 shows the path through reciprocal space of the tip of the diffraction vector $\mathbf{S}$ as the angular position of the detector is varied. For large $|\mathbf{S}|$, changes in the scattering angle 2θ are taken as a measure of $|S_{||}-G_{||}|$. The resulting error is less than a few percent even at the Brillouin zone boundaries. However, the path of the tip of the scattering vector is not normal to the reciprocal lattice rod and so the intensity modulation along the rod will affect the diffuse intensity. This effect is more serious for large angles between the incident beam and the crystal normal. To minimize this effect,

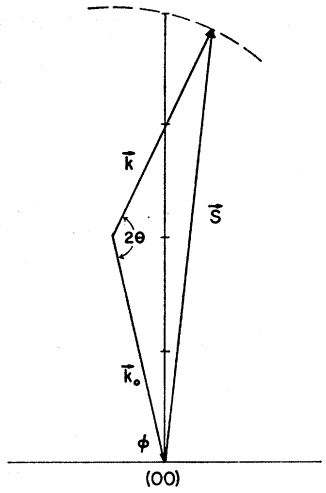

FIG. 2. Geometry of a scattering experiment near the (00) reciprocal-lattice rod. The dotted line is the path of the detector when 2θ is changed.

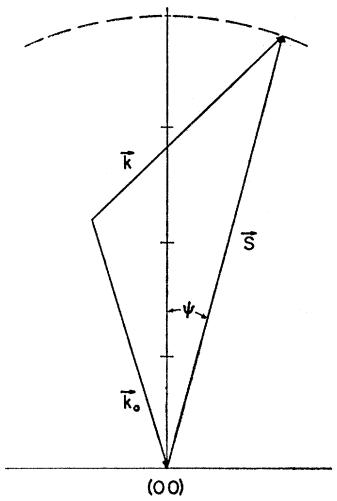

FIG. 4. Geometry of a scattering experiment near the (00) reciprocal-lattice rod. The triangle $\mathbf{k}$, $\mathbf{k}_0$, and $\mathbf{S}$ is kept rigid while ψ is varied by tilting the crystal. The dotted line is the path of the detector.

the data to be presented here were taken with the detector crossing the rods at positions of intensity maxima due to the residual third Laue condition.

Figure 3 shows a log-log plot of the intensity as a function of detector angle for the (444) diffraction peak, which is on the (00) reciprocal-lattice rod. The angle of incidence was 81° and the energy was 94 eV. The circles and crosses refer to opposite sides of the peak. While the slope of the wings is nearly -1, there is considerably asymmetry. This asymmetry will be discussed first.

Beside the $|S_{||}-G_{||}|^{-1}$ factor, there is an angular dependence in Eq. (6) arising from $|f_0|^2$. There may be additional angular dependences outside the scope of the simple model. In order to study the thermal diffuse scattering alone, it is desirable to eliminate effects due to $|f_0|^2$. This can be accomplished by taking data in a way that holds the scattering angle 2θ constant. Figure 4 shows the geometry of such an experiment. The rigid triangle composed of $\mathbf{k}_0$, $\mathbf{k}$, and $\mathbf{S}$ is rotated by tilting the crystal. The angle ψ is a measure of $|S_{||}-G_{||}|$. An example of data taken in this way is shown in Fig. 5. The wings are symmetric to within experimental error, which is true for all data taken across the (00) rod.

This method of taking data requires that $I_0(\mathbf{S})$ not be a rapid, explicit function of the angle of incidence. Many experiments show that the intensity along the reciprocal-lattice rods depends sensitively on the angle of incidence, but in these experiments the scattering angle must be changed also and there is no way of separating the dependences. In the present experiments the observed symmetry indicates no explicit dependence of $I_2(\mathbf{S})$ on the angle of incidence. Incidentally, this result suggests that by comparing the diffuse intensities measured in the two types of experiments one might measure the angular dependence of $|f_0|^2$ and investigate to what extent a kinematic theory involving a structure factor is valid for describing low-energy electron diffrac-

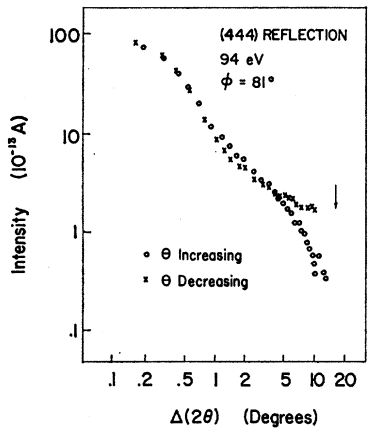

FIG. 3. Scattered intensity versus $\Delta(2\theta)$. The detector crosses the (00) rod at the (444) reflection. The crosses and dots indicate data taken on opposite sides of the rod. The vertical arrow indicates the zone boundary. The data are for 22°C.

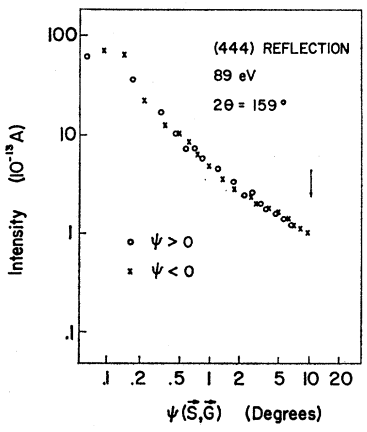

FIG. 5. Scattered intensity versus ψ. The tip of $\mathbf{S}$ crosses the (00) rod at the (444) reflection. The crosses and dots indicate data taken on opposite sides of the rod. $T=22$°C.

tion. Experiments exploring this possibility are now in progress.

In Fig. 5 the slope is not constant but decreases toward the zone boundary. This is due to a temperature-independent background. Figure 6 shows the intensity on a linear plot for two different temperatures. While both the Bragg peak and diffuse wings show a definite temperature dependence, the scattered intensity near the zone boundary is essentially constant and independent of temperature. Data for intermediate temperatures fall between these curves and have the same value at the zone boundary. When this background is subtracted from the data, curves as in Figs. 7(a) and 7(b) result. The solid line is ψ^{-1} and the dashed line is a plot of Eq. (6).

We have investigated the effect of the finite detector aperture on the observed angular dependence of the scattering. Although slit corrections cannot be made accurately since the electron optics of the detector are not well known, we have estimated the corrections based on the geometrical aperture, and found them less than 2% everywhere outside of the Bragg peak itself.

We have also considered the effect of the finite breadth of the individual phonon side bands on the observed angular dependence. Integrating over a family of side bands each assumed to be Lorentzian with a half-width of 0.25° and with an intensity proportional to $|\mathbf{q}|^{-1}$ gives a resulting angular dependence indistinguishable from ψ^{-1} except within the Bragg peak itself. This assumed side-band width is of the order of that of the Bragg peak and is also consistent with a typical phonon mean free path of a few hundred angstroms.

We thus conclude that throughout most of the Brillouin zone the angular dependence is consistent with the simple model of the previous section. Unfortunately, near the zone boundary where the phonon dispersion relation for the discrete lattice would differ from that for the continuum, the experimental uncertainties are large since the thermal diffuse intensity is comparable to or less than the temperature-independent background. It is also here that the difficulties due to the finite penetration of the electrons into the crystal will be most important.

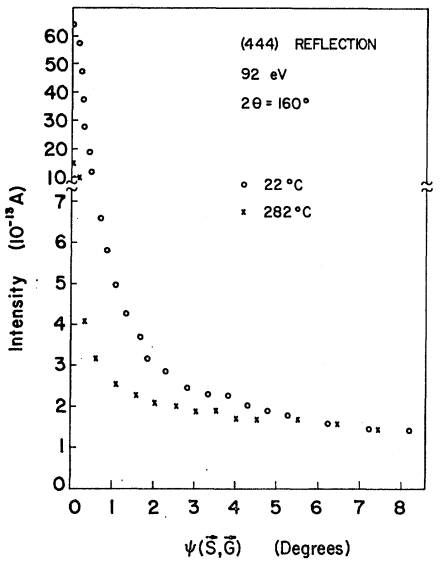

FIG. 6. Scattered intensity versus ψ at two different temperatures. Data taken at intermediate temperatures fall between these curves and give the same temperature-independent background.

Dependence on Temperature and $|\mathbf{S}|$

We now discuss the temperature dependence of the scattering. The data are presented in Fig. 8. Here the ratio of the diffuse intensity at $q_{||}=\pi/4d$ to the intensity at the maximum of the diffraction peak is plotted as a function of temperature for several reflections. The temperature-independent background has been subtracted. Within the uncertainties the intensity ratios are proportional to the temperature, as expected from Eq. (6). There is considerable scatter in the data for the lowest-order reflection, where the thermal diffuse

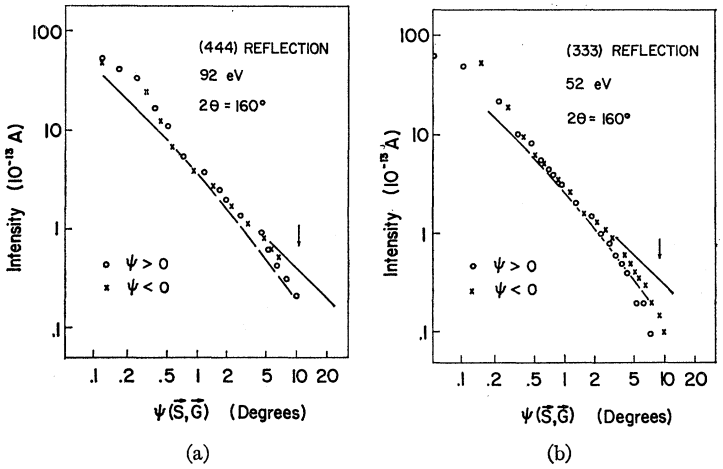

FIG. 7. Scattered thermal diffuse intensity versus ψ. (a) (444) reflection; (b) (333) reflection. The temperature-independent background has been subtracted. The straight line has slope -1; the dashed curve is a plot of Eq. (6).

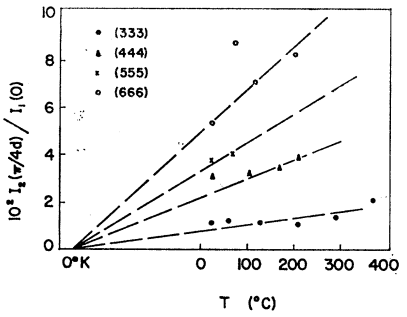

FIG. 8. Temperature dependence of the thermal diffuse scattering. $I_2(\pi/4d)/I_1(0)$ is plotted as a function of temperature for various reflections on the (00) reciprocal-lattice rod. The background has been subtracted. The lines are fits through the origin.

scattering is very small and somewhat difficult to distinguish from the central diffraction peak even a fourth of the way to the zone boundary. For the highest-order reflection, large uncertainties arise because the intensities are low due to the Debye-Waller factor, and the background is a relatively large correction.

Equation (6) also predicts that this same ratio should be proportional to $|\mathbf{S}|^2$. This feature can be checked by plotting the slopes of the lines in Fig. 8 against the magnitude of $\mathbf{S}$ for the various reflections. This is shown in Fig. 9, where the straight line is the predicted $|\mathbf{S}|^2$.

Integrated Intensity

According to Eq. (11), the ratio of the integrated intensity in the thermal diffuse scattering and that in the associated Bragg peak should be nearly $2M$, the exponent in the Debye-Waller factor. This ratio is difficult to determine experimentally. There is ambiguity in separating the wings of the diffraction maxima from the thermal diffuse scattering near the center of the zone; the thermal diffuse scattering is not accurately known near the zone boundary; and the electron optics of the apparatus are not well known.

We examine the intensities for the (444) reflection. The energy is 91 eV. For this reflection the measured effective Debye temperature is 160°K,[1] which gives $2M=1.45$ at 300°K.

To determine the integrated thermal diffuse intensity we assume that it has a ψ^{-1} dependence throughout the entire Brillouin zone and we neglect the variation in the electron flux over the solid angle subtended by the detector slit. The latter is a good approximation since the diffuse intensity is slowly varying. Uncertainty in the background correction is the major source of error and in this case may be as large as 9% of the integrated current. For this reflection

$$\int_{\text{zone}} I_2(\mathbf{S})d\Omega = 12.9\times10^{-11}\ \text{A}.$$

The intensity in the Bragg peak is very uncertain because neither the detector optics nor the shape of the perfect collimation diffraction maximum is exactly known. We therefore make two estimates, first assuming a Gaussian and then a Lorentzian shape. These assumptions will under- and overestimate the intensity, respectively. In view of this large uncertainty, no serious additional error is made by assuming that the detector aperture is narrow compared to the width of the peak. Then, for a slit width $\Delta\psi$ and a slit height $\Delta\xi$, and for a Gaussian peak, the observed current is

$$I(\psi)=\Delta\psi\int_{-\Delta\xi/2}^{\Delta\xi/2} Ce^{-b(\psi^2+\xi^2)}d\xi. \qquad (12)$$

b is determined by the best fit of a Gaussian to the data. The effective aperture of the detector is smaller than the actual dimensions of the slit because of the bias fields necessary for energy selection. This effect is small, and the physical dimensions of the slit are used in Eq. (12). The integration gives a value of C from which the integrated intensity in the Bragg peak is found directly. For this reflection

$$\int_{\text{zone}} I_1(\mathbf{S})d\Omega = 2.77\times10^{-11}\ \text{A}.$$

Thus the ratio

$$R=\frac{\int_{\text{zone}} I_2(\mathbf{S})d\Omega}{\int_{\text{zone}} I_1(\mathbf{S})d\Omega}=4.7=3.2(2M).$$

An entirely similar estimate for a Lorentzian line shape gives

$$\int_{\text{zone}} I_1(\mathbf{S})d\Omega = 17\times10^{-11}\ \text{A}$$

and

$$R=0.76=0.53(2M).$$

Thus the two results bracket the value expected from Eq. (11), and within the large uncertainty the results are in agreement with the expectations of the simple model.

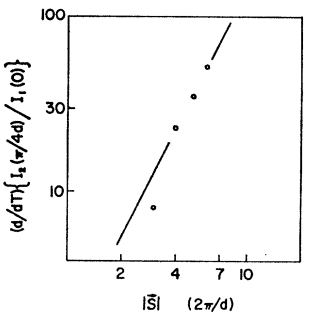

FIG. 9. Dependence of the thermal diffuse scattering on the magnitude of $\mathbf{S}$. The slopes of the lines in Fig. 8. are plotted versus $\mathbf{S}$. The slope of the straight line is 2.

MODIFICATIONS OF THE SIMPLE MODEL

The agreement between the experimental results and the expectations of the simple model demonstrates that the observed intensity is indeed the thermal diffuse scattering. This is the main conclusions of this paper. However, even in the framework of the kinematic theory, the model is deficient in two important ways. First, it has neglected the finite penetration of the elastically scattered electrons, and second, it has not treated the force-free elastic boundary conditions carefully. Before experiments such as these can give detailed information about the surface lattice dynamics, these effects must be understood. We now discuss each of them briefly.

Effects of Electron Penetration

We begin the discussion of the effects of the electron penetration by rewriting Eq. (1).

$$I_2(\mathbf{S})=\sum_{ij} a_i a_j e^{i\mathbf{S}\cdot(\mathbf{r}_i-\mathbf{r}_j)} e^{-\frac{1}{2}\langle(\mathbf{S}\cdot\mathbf{u}_i)^2\rangle} \times e^{-\frac{1}{2}\langle(\mathbf{S}\cdot\mathbf{u}_j)^2\rangle}\langle(\mathbf{S}\cdot\mathbf{u}_i)(\mathbf{S}\cdot\mathbf{u}_j)\rangle, \quad (13)$$

where a_i is the amplitude scattered by the ith atom. We change the summation indices from i and j to ln and $l'n'$, where n labels a plane parallel to the surface and l labels an atom in the plane, and use the results of I to obtain the a_i's. There the attenuation of the beam of coherent electrons was accounted for by a linear absorption coefficient so that the ratio of the amplitudes scattered by atoms in successively deeper planes is a constant α. Thus $a_{ln}=f_0\alpha^n$ for unit incident intensity. The Debye–Waller factors $e^{-\frac{1}{2}\langle(\mathbf{S}\cdot\mathbf{u}_i)^2\rangle}$ are the same for atoms in a given plane and are written as $\gamma_{n\mathbf{S}}$. These are evaluated from Eq. (4) of I. Thus

$$I_2(\mathbf{S})=|f_0|^2\sum_{ln}\sum_{l'n'}\alpha^n\alpha^{n'}\gamma_{n\mathbf{S}}\gamma_{n'\mathbf{S}}e^{i\mathbf{S}\cdot(\mathbf{r}_{ln}-\mathbf{r}_{l'n'})} \times\langle(\mathbf{S}\cdot\mathbf{u}_{ln})(\mathbf{S}\cdot\mathbf{u}_{l'n'})\rangle. \quad (14)$$

Incidentally, it is interesting to note that for large $|\mathbf{S}|$ the effect of $\gamma_{n\mathbf{S}}$ is large, and for example, for the (666) reflection the amplitude scattered by the second layer is greater than that scattered by the first.

It is now necessary to expand the u_{ln}'s in the normal modes of the system. One should use the modes arising from complete treatment of the force-free boundary conditions. This would be a formidable computational task not warranted in the present treatment. To display the quantitative results to be expected, we approximate the effect of the boundary conditions in two different ways. In the first we require that modes with normal components of their wave vectors equal to $\pm q_\perp$ combine to give an antinode at the surface. Thus

$$(\mathbf{u}_i)_{\mathbf{q}z}=2\mathbf{e}_{\mathbf{q}z}u_{\mathbf{q}z}\sin(q_{||}r_l+\omega t+\delta_{\mathbf{q}z})\cos q_\perp r_n, \quad (15)$$

where r_l and r_n are the parallel and normal components of r_{ln}. This is appropriate for transverse bulk modes with $\mathbf{e}_{\mathbf{q}z}$ in the plane of the surface. Actually, such modes would give no contribution to the diffuse scattering near the (00) reciprocal-lattice rod because of the factor $(\mathbf{S}\cdot\mathbf{e}_{\mathbf{q}z})$. However, we continue with the approximation since it should contribute to a qualitative understanding of the effects of the electron penetration from combinational modes where $(\mathbf{S}\cdot\mathbf{e}_{\mathbf{q}z})\neq 0$. Using Eq. (15),

$$\langle(\mathbf{S}\cdot\mathbf{u}_{ln})(\mathbf{S}\cdot\mathbf{u}_{l'n'})\rangle=4\sum_{\mathbf{q}}(\mathbf{S}\cdot\mathbf{e}_{\mathbf{q}z})^2\langle u_{\mathbf{q}z}^2\rangle \times\cos(q_\perp r_n)\cos(q_\perp r_{n'})\cos[q_{||}(r_l-r_{l'})]. \quad (16)$$

Substituting Eq. (16) into Eq. (14) gives

$$I_2(\mathbf{S})=|f_0|^2\sum_{\mathbf{q}z}(\mathbf{S}\cdot\mathbf{e}_{\mathbf{q}z})^2\sum_{nn'}\alpha^n\alpha^{n'}\gamma_{n\mathbf{S}}\gamma_{n'\mathbf{S}} \times e^{-iS_\perp(r_n-r_{n'})}\langle u_{\mathbf{q}z}^2\rangle\cos(q_\perp r_n) \times\cos(q_\perp r_{n'})\{\sum_{ll'}e^{-i[(\mathbf{S}+\mathbf{q})_{||}(r_l-r_{l'})]}\}. \quad (17)$$

The term in braces gives a contribution only from phonons for which $S_{||}+q_{||}=G_{||}$. We consider the diffuse intensity only on a plane normal to the reciprocal-lattice rod at a point satisfying the third Laue condition so that $e^{-iS_\perp(r_n-r_{n'})}=1$. We now replace $\langle u_{\mathbf{q}z}^2\rangle$ by its value for a Debye spectrum in the high-temperature limit, change the summation over $\mathbf{q}z$ into an integral, and perform the integration. This gives

$$I_2(\mathbf{S})=\frac{N\pi dkT}{24mc^2}\frac{|f_0|^2|\mathbf{S}|^2}{q_{||}}\sum_n\sum_{n'}\alpha^n\alpha^{n'}\gamma_{n\mathbf{S}}\gamma_{n'\mathbf{S}} \times\{e^{-d(n+n')q_{||}}+e^{-d(n-n')q_{||}}\}. \quad (18)$$

Now $I_2(\mathbf{S})$ can be evaluated numerically for various values of $q_{||}$. The resulting angular dependence of the thermal diffuse scattering is shown as curve 1 in Fig. 10.

As the second approximate way of treating the force-free boundary condition, we consider modes whose amplitudes fall exponentially with depth. This is an appropriate approximation for Rayleigh surface waves. Then

$$(\mathbf{u}_i)_{\mathbf{q}z}\langle u_{\mathbf{q}z}^2\rangle=\mathbf{e}_{\mathbf{q}z}\sin(q_{||}r_{||}+\omega t+\delta)e^{-\epsilon|\mathbf{q}|nd}, \quad (19)$$

where ϵ is chosen to be $\frac{1}{2}\pi$ so that the amplitude falls to $1/e$ in a depth equal to a wavelength. $\langle u_{\mathbf{q}z}^2\rangle$ is proportional to $|\mathbf{q}|^{-1}$ so that each mode has the same energy kT. Using Eq. (19), $I_2(\mathbf{S})$ is calculated just as for the previous approximation except that there is no integration over $q_\perp$. The results are shown as curve 2 in Fig. 10.

Surface modes, even in the continuum approximation, are more complicated than was assumed in Eq. (19) and consist of two elliptically polarized components with different exponential damping factors.[7] The complete

[7] L. D. Landau and E. M. Lifschitz, *Theory of Elasticity* (Addison-Wesley Publishing Company, Reading, Massachusetts, 1959).

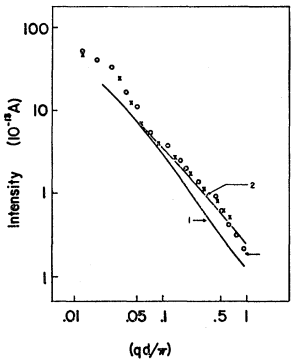

FIG. 10. Effect of the electron penetration on the angular dependence of the thermal diffuse scattering. Curve 1 is a plot of Eq. (18), which assumes antinodes of the elastic waves at the free surface. Curve 2 is calculated for an exponential decay of the vibrational amplitude with depth. The data points are for the (444) reflection at 22°C.

expression for surface waves in a continuum with parameters appropriate for silver were used to calculate $I_2(\mathbf{S})$ at the origin and at the zone boundary. The result is indicated by the horizontal arrow in Fig. 10 and suggests that the use of Eq. (19) does not lead to a large error in the angular dependence of $I_2(\mathbf{S})$.

A more correct calculation using the result of Refs. 5 or 6 would presumably give an angular dependence of $I_2(\mathbf{S})$ similar to some linear combination of curves 1 and 2. These approximate treatments of the electron penetration cause $I_2(\mathbf{S})$ to fall below ψ^{-1}. This is expected in view of the difference between the thermal diffuse scattering from two and three dimensional structures. The phonon dispersion for the discrete lattice will differ from the continuum in the outer part of the zone and there give a diffuse intensity lying above ψ^{-1}, or an effect opposite to that of the electron penetration. From this discussion it is clear that no detailed information about the phonon dispersion relation in the discrete lattice can be obtained until the electron penetration is known in detail.

Another interesting feature arises in the discussion of the penetration. Because of the larger vibrational amplitudes of the surface atoms, the diffuse scattering "sees" the surface layer even more strongly than the Bragg scattering does. This is illustrated by comparing values of the sums of Eq. (18) and Eq. (5) of I with their values when only the terms with $n=n'=0$ are retained. Such a comparison shows that the surface layer contributes proportionately about twice as much to the diffuse intensity at the zone boundary as it does to the Bragg scattering. This changes the ratio of the expected integrated intensities by less than a factor of 2.

Comparison with Theory and Discussion

One would like to compare the experimental observations of the diffuse scattering with the theoretical calculations of Huber[5] and of Wallis and Maradudin,[6] which take explicit account of the force-free elastic boundary conditions. Neither is strictly comparable with experiment because they consider scattering by the outermost atomic layer only, but there is general agreement in that both calculations predict the ψ^{-1} dependence near the reciprocal-lattice rods. Unfortunately, experimental limitations prevent many more detailed comparisons. As has been pointed out, no precise information about the phonon dispersion in the discrete lattice is available, and the experiments agree equally well with both the continuum and lattice calculations.

Both calculations predict anisotropies in the diffuse scattering around reciprocal-lattice rods other than (00). These arise from anisotropy in the sound velocity and from the polarization factor $(\mathbf{S}\cdot\mathbf{e}_{qz})$. Although these anisotropies should be measurable, they are not in the present experiments because of the detector geometry and because of the large uncertainty in comparisons of absolute intensities after reorientation of the crystal. The experimental result that the diffuse scattering is the same on opposite sides of the (00) rod does, however, establish that the iso-diffusion surface is at least 6-fold symmetric. Comparison of intensities at the same ψ but various crystal azimuths indicate the peak to valley ratio of any 6-fold variation about the (00) rod is less than 1.5.

A somewhat more interesting comparison can be made concerning the magnitude of the diffuse intensity where there is a discrepancy between the two model calculations.[5] Huber's calculation for the elastic continuum predicts that the diffuse scattering from the outermost atomic plane should be roughly twice what it would be if the thermal motions of the surface were the same as in the bulk. This agrees with our Eq. (11) where the value of $2M$ is that for the surface and equal to approximately twice the bulk value. Wallis's and Maradudin calculation predicts an intensity about half this large. The experimental result from above is $0.52(2M)<R<3.2(2M)$ where $2M$ is the measured low-energy electron value. The lower limit of this range just includes the Wallis and Maradudin value, but the experiment seems to favor Huber's result.

ACKNOWLEDGMENTS

The authors would like to thank D. L. Huber for many helpful discussions and suggestions about the analysis and interpretation of this work. We would also like to thank M. G. Lagally for his assistance.